Identification of the Carbon Dangling Bond Center at the 4*H*-SiC/SiO_2 Interface by an EPR Study in Oxidized Porous SiC

J. L. Cantin,[1] H. J. von Bardeleben,[1] Y. Shishkin,[2] Y. Ke,[2] R. P. Devaty,[2] and W. J. Choyke[2]

[1]*Groupe de Physique des Solides, Universités Paris 6&7, UMR 7588 au CNRS, 2, place Jussieu, 75005 Paris, France*
[2]*Department of Physics and Astronomy, University of Pittsburgh, Pittsburgh, Pennsylvania 15260, USA*
(Received 24 July 2003; revised manuscript received 16 September 2003; published 8 January 2004)

We report the observation of a paramagnetic interface defect in thermally oxidized porous *n*-type doped 4*H*-SiC/SiO_2. Based on its axial symmetry and resolved hyperfine interactions it is attributed to an sp^3 carbon dangling bond center situated at the SiC side of the interface. This center is electrically active and pins the Fermi level in the oxidized samples. No silicon related paramagnetic dangling bond centers are observed. The formation of dangling bond centers seems to be related to interstitial oxygen diffusion at the interface during the oxidation process.

DOI: 10.1103/PhysRevLett.92.015502 PACS numbers: 61.72.Ji, 68.35.Dv, 73.20.Hb

The modeling and experimental investigation of the microscopic structure of the interface between a crystalline semiconductor and its amorphous oxide are challenging tasks [1,2]. Recently the thermal oxidation of SiC and the structure of the SiC/SiO_2 interface have attracted much interest [3–6] due to the increased complexity as compared to the Si/SiO_2 case and the practical applications predicted. One major problem for the modeling of the thermal oxidation process is the determination of the atomic scale mechanisms, which will lead to the required oxygen incorporation and the CO emission. Experimental information on these processes is still very limited and additional experiments are clearly required. We know from nuclear reaction analysis that the interface reaction between oxygen and SiC is the limiting step in the oxidation process [7]. This leads to very different oxidation kinetics for the C(000-1) and Si(0001) interfaces contrary to the Si case where the oxygen diffusion through the SiO_2 layer is the limiting process. Positron annihilation spectroscopy has shown the presence of open volume defects at the oxygen side of the SiC/SiO_2 interface [8], which implies the presence of interface defects at the SiC side. However, no direct experimental evidence of their microscopic structure has been reported up to now.

High concentration of electrically active interface defects have been evidenced by electrical measurements. The D_{it} concentrations at both the conduction and valence band edges are typically $10^{13}/\mathrm{cm}^2\,\mathrm{eV}$ [9], which is an order of magnitude higher than in the case of Si/SiO_2. Worse, whereas hydrogen passivation allows to reduce D_{it} to acceptable values of below $10^{11}\ \mathrm{cm}^{-2}$ for Si/SiO_2, no efficient passivation has been obtained up to now for the SiC/SiO_2 interface [10]. Therefore device applications of SiC/SiO_2 metal-oxide-semiconductor field-effect transistor (MOSFET) structures are still rare.

Up to now electron paramagnetic resonance (EPR) spectroscopy, the technique of choice for interface defect studies, has not been successful for the SiC/SiO_2 case. In the case of (100)Si/SiO_2 interfaces it has been decisive for the identification of the two main interface defects, P_{b0} and P_{b1}, attributed to threefold coordinated Si dangling bond centers (P_{b0}) and partially oxidized Si-Si dimer interface defects (P_{b1}), respectively [11,12]. In spite of various attempts, no oxidation related defect has been observed in 3C-, 4*H*-, and 6*H*-SiC. Only a post oxidation high temperature annealing induced isotropic defect, attributed to carbon dangling bonds in the oxide, has been reported [13]. These negative results seem to contradict the electrical measurements.

We have recently shown that oxidized porous silicon can be extremely useful for interface defect studies. One remarkable finding was that due to faceting (111) and (100) surfaces are largely predominating irrespective of the particular pore structure. In *n*-type 4*H*-SiC, a triangular pore structure can be obtained in which the external (0001) face is the dominant internal surface [14]. Most of our samples presented this pore structure. Because of the much higher internal surface area as compared to the external surface—it is typically of the order of $100\ \mathrm{m}^2/\mathrm{cm}^3$ in porous Si—much higher sensitivities for EPR studies can be achieved. The high signal to noise ratio obtainable with porous samples is particularly important for the detection of the low intensity hyperfine lines, which are key elements for modeling of the defect structures. EPR studies of porous oxidized Si allowed, for example, the first determination of the g tensor of the P_{b1} center [15] and the first electron nuclear double resonance (ENDOR) measurement on the P_{b0} center [16]. We have therefore applied the same approach to the case of SiC, and we present in this Letter the results of an EPR study of thermally oxidized porous 4*H*-SiC layers.

Porous SiC layers of thickness between 5 and 100 μm were prepared by photoelectrochemical dissolution from standard (0001) 4*H*-SiC:N substrates with 3.5° or 8° off axis orientation. Both supported and freestanding porous layers have been studied. The samples were thermally oxidized at 1000 °C in dry oxygen at low pressure (23 mbar) in a closed furnace. The EPR measurements

 0031-9007/04/92(1)/015502(4)$20.00 © 2004 The American Physical Society

were performed at 35 and 9 GHz in the 4 to 300 K temperature range. The angular variation of the spectra has been observed for a rotation of the magnetic field in the (11-20) and (1-100) planes. Because of the only partial resolution of the observed multiline spectrum, a computer-assisted decomposition has been performed.

After the oxidation, all samples presented independently of the initial doping and the dissolution conditions a high intensity anisotropic multiline spectrum. In Fig. 1 we show typical EPR spectra measured at 35 GHz for different magnetic field orientations. These spectra are not observed in bulk samples submitted to the same treatment. From their angular dependence, reflecting the crystal structure of 4H-SiC, we can conclude that the defects at the origin of these spectra are not located in the amorphous SiO_2 layer either. We will show in the following analysis that the spectra must be attributed to defects located on the crystalline SiC side of the interface.

As the individual components of the EPR spectrum are only partially resolved a computer-assisted decomposition of the multiline spectrum has been performed. The EPR spectra are best resolved for the high symmetry orientations: for $B//c$ the spectrum can be decomposed in two lines, for $(B, c) = 54°$ into three lines, and for $B \perp c$ into three lines. A small intensity isotropic line at $g = 2.0028$ is equally present but it will no longer be discussed in this Letter. Such angular variation would be expected for a spin $S = 1/2$ center with an axially symmetric g tensor oriented parallel to the nearest neighbor (NN) directions. Carbon or silicon dangling bond centers are good candidates for such defects. For a C or Si dangling bond center oriented parallel to the c axis, a C_{3v} symmetry can be expected. Because of the wurtzite structure of 4H-SiC, the symmetry will be lowered to C_{1h} for a dangling bond defect oriented along the other NN directions. We will neglect the difference between the two inequivalent (k, h) lattice sites, which concerns only second nearest neighbor configurations. Therefore, for a rotation of the magnetic field in the (1-100) plane, five distinguishable differently oriented centers will be expected for 4H-SiC, which degenerate for special high symmetry directions (Fig. 2) into two branches (for $B//[0001]$) and into three branches (for B at 90° from c axis). Simulations of the angular variations within this model are in good agreement with the experimental results.

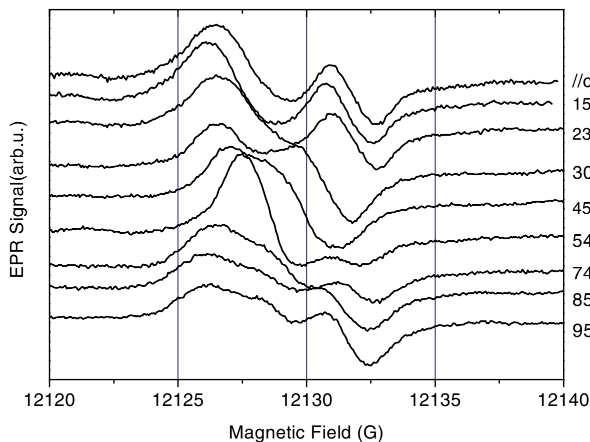

FIG. 1 (color online). Q-band (35 GHz) EPR spectra observed in porous 4H-SiC/SiO_2 for various magnetic field orientations relative to the c axis; the rotation plane is (1-100), $T = 300$ K.

The angular dependence of the EPR spectra can be described by the following spin Hamiltonian for $S = 1/2$:

$$\mathbf{H} = \mu_\mathbf{B} \mathbf{B} \cdot \mathbf{g} \cdot \mathbf{S} + \sum_i \mathbf{S} \cdot \mathbf{T}^i \cdot \mathbf{I} + \mathbf{S} \cdot \mathbf{A} \cdot \mathbf{I},$$

where all symbols have their usual meaning. **T** and **A** are the superhyperfine (SHF) and central hyperfine (HF) interaction tensors.The principal values of the g tensors of the on c-axis and off c-axis centers, respectively, can be deduced from this decomposition; they are $g_{//c} = 2.0023$ and $g_{\perp c} = 2.0032$ and $g_{xx} = 2.0031$, $g_{yy} = 2.0028$, and $g_{zz} = 2.0023$.

To distinguish between carbon and silicon dangling bond centers, which can both be expected at the SiC/SiO_2 interface, information on the central and superhyperfine interactions is required. Fortunately, such interactions are indeed observed; they have been analyzed at X-band frequency, where the SHF lines are well separated from the central part of the spectrum. In Fig. 3 we show a typical spectrum for $B//c$ at a larger scale: two low intensity lines with an approximate splitting of about

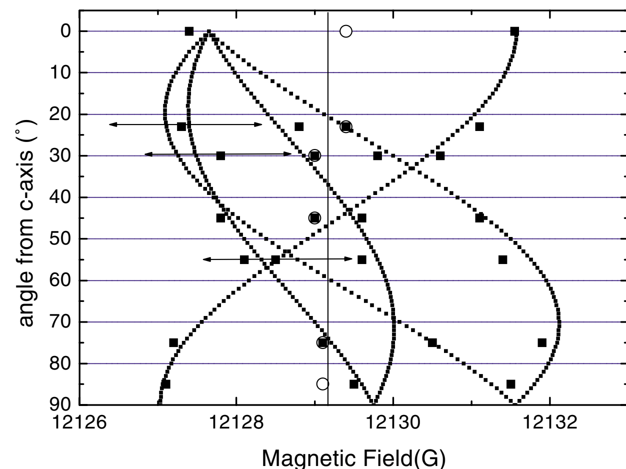

FIG. 2 (color online). Simulated (small dots) and experimental (squares) angular dependence of the carbon Pb center spectrum in porous 4H-SiC/SiO_2 for a rotation in the (1-100) plane; an additional small intensity isotropic line at $g = 2.0028$ is equally indicated (circles). Because of the linewidth of 2 G the low field part of the spectrum was simulated by one average line for some orientations as indicated by arrows

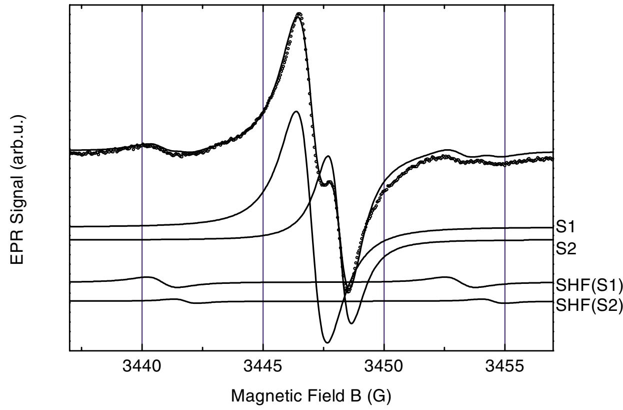

FIG. 3 (color online). EPR spectrum of $4H$-SiC/SiO$_2$ for $B//c$ and its decomposition into two central lines $S1$, $S2$ and their respective superhyperfine doublets SHF($S1$), SHF($S2$).

13 G are observed symmetrically about the central part of the spectrum. The decomposition of the spectrum shows that the HF structure is composed of four lines, i.e., one hyperfine doublet associated with each central line. The splittings are 12.4 and 13.0 G, respectively, which gives $T_{//c} = 13.0$ G. At still higher gain additional lines are observed at twice the distance from the central lines; they correspond to the presence of two nuclei with $I \neq 0$ in the nearest neighbor (NN) shell. Their observation demonstrates directly that these doublets result from the hyperfine interaction with ligand atoms and are not due to hyperfine interaction with the central nucleus. The superhyperfine interaction is only slightly anisotropic with splittings varying between 12 and 13 G. Because of the limited resolution of the EPR spectroscopy ENDOR measurements will be required to establish the complete angular variation of the SHF tensor.

The nature and number of the ligand atoms can be determined from the intensity ratio between the central line and the SHF lines. As the isotope abundances of Si and C nuclei with a nonzero spin are different [^{29}Si ($I = 1/2$), 4.7% and ^{13}C ($I = 1/2$), 1.1%], they will give rise to SHF spectra with distinct intensity ratios. Assuming identical line shapes and widths for the central and SHF lines, we determine an intensity ratio I(SHF lines)/I(central line) of $\sim$0.10. As the HF lines are slightly broader than their central line, their intensity is underestimated. The ratios expected for the case of 3 Si neighbors or 3 C neighbors are 0.146 and 0.033, respectively. We thus attribute the SHF interaction to a shell of three equivalent Si neighbors. This is the expected configuration of a C dangling defect interacting with the first nearest Si neighbors (NN).

A further direct test for the Si or C nature of the dangling bond center is the observation of the central hyperfine interaction. At 25 times higher gain than the one used to measure the central lines, we observe additional weak structures, symmetrical to the center part

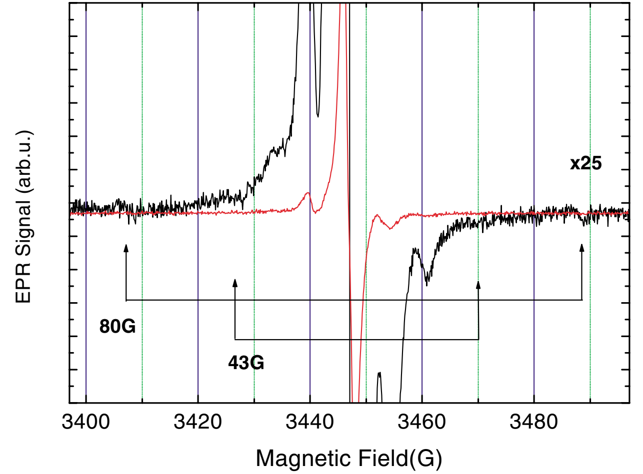

FIG. 4 (color online). High gain ($\times$ 25)EPR spectrum for $B//c$, displaying the central hyperfine lines with splittings of 80 and 43 G and the central part ($\times$ 1).

(Fig. 4). We observe for $B//c$ one doublet with a splitting of 80 G and a linewidth of 2 G as well as a broader doublet with a splitting of 43 G. Assuming the central hyperfine interaction tensor $\mathbf{A}$ to be axially symmetric, we can deduce from these two values the principal values $A_{//} = 73 \times 10^{-4}$ cm^{-1} and $A_{\perp} = 35 \times 10^{-4}$ cm^{-1}. The intensity ratio I(HF lines)/ I(central lines) is close to 1%, identifying it as the central HF interaction with a ^{13}C nucleus. Thus, we attribute the defect to a carbon dangling bond center. Based upon its similarities to the P_{b0} center, we name it P_{bC} center.

One of the fingerprints of interface defects is a g-factor distribution related to the varying local environments; this has been previously observed for the Pb centers at the Si/SiO$_2$ interface. If the linewidth is predominantly determined by the g-factor distribution, it will increase linearly with the microwave frequency whereas the width of inhomogeneously broadened lines, the normal case of point defects in SiC, is independent of the frequency. We have therefore measured the linewidth of the P_{bC} center at 35 and 9.6 GHz. A typical result for $B//c$ is shown in Fig. 5: we observe for the high field line a peak to peak width of 0.7 G at 9.6 GHz which increases to 2.1 G at 35 GHz. This result gives further clear support for the interface defect model.

The spin localization can be deduced from the central hyperfine $\mathbf{A}$ tensor $\mathbf{A}$ after decomposition into an isotropic part $a\mathbf{I}$ and an anisotropic part $\mathbf{b}$ according to $\mathbf{A} = a\mathbf{I} + \mathbf{b}$:

$$a = (1/3)(A_{//} + 2A_{\perp}) = (2/3)\mu_0 g \mu_B g_N \mu_N \eta^2 \alpha^2 |\Psi_S(0)|^2,$$

$$\begin{aligned} b &= (1/3)(A_{//} - A_{\perp}) \\ &= (1/4\pi)\mu_0 g \mu_B g_N \mu_N \eta^2 \gamma^2 (2/5)\langle r^{-3}\rangle_p. \end{aligned}$$

The principal values of $\mathbf{b}$ are ($-2b, b, b$) and $\eta^2\alpha^2$ and

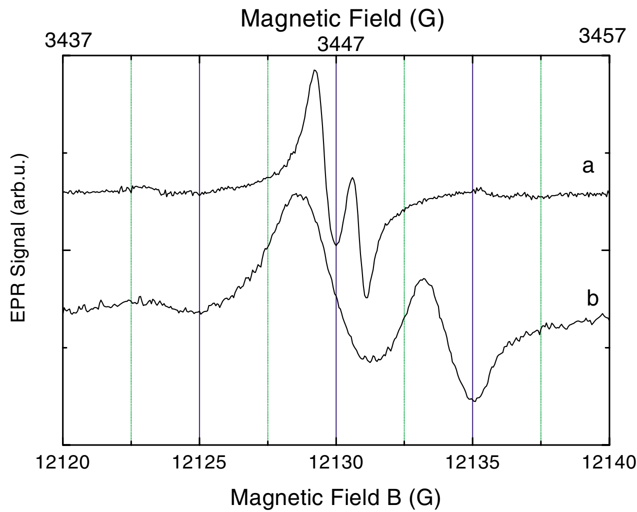

FIG. 5 (color online). Comparison of the EPR linewidth at 9.6 GHz (upper scale) and 35 GHz (lower scale) for $B//c$; in both cases the scale is 20 G

$\eta^2\gamma^2$ are the spin densities in the C $2s$ and $2p$ orbitals (for further definitions, see [17]). We obtain $a = 48 \times 10^{-4}$ cm^{-1} and $b = 13 \times 10^{-4}$ cm^{-1}. Using the atomic constants given by Morton and Preston [18] we can determine the s and p spin densities: $\eta^2\alpha^2 = 4\%$ and $\eta^2\gamma^2 = 35\%$. The s/p ratio, which is $1/3$ for a perfect sp^3 dangling bond defect [17], is only 0.11; this indicates a relaxation of the carbon atom from the tetrahedral position towards a planar configuration. The angle θ between the dangling bond and the backbonds can be estimated in a simple model [19] from the expression $\tan\theta = -[2(1 + \gamma^2/\alpha^2)]^{1/2}$; this gives $\theta = 102°$. The spin distribution is more delocalized for the P_{bC} center (60% on the neighbor atoms) than for the P_{b0} center (30%).

In conclusion, we report the observation of a carbon dangling bond center at the $4H$-SiC/SiO$_2$ interface. Such centers may be considered as "natural" reliquats of the oxidation process in the spirit of the model of Ref. [3] developed for cubic SiC: the initial step of oxidation is the incorporation of atomic oxygen as an interstitial in a Si-C bond at the interface with subsequent diffusion in the (112) plane parallel to the interface plane. When oxygen atoms switch from one C-O-Si-C configuration to the neighboring C-Si-O-C one, dangling bond defects are generated if the reformation of Si-C bonds after the ejection of a O atom is incomplete. Experimental support for the presence of remaining interface C-O-Si bonds in oxidized $4H$-SiC the has been given by photoelectron emission spectroscopy [20]. *A priori*, the formation of Si dangling bond centers might also be expected. Their nonobservation in our EPR study does not demonstrate that they are absent. In fact, their nonobservation might be related to an inadequate Fermi-level position as only positively charged Si dangling bond centers are EPR active.

We thank DURINT (Grant No. N00014-01-1-0715) for partial support of the work at the University of Pittsburgh.

[1] A. Pasquarello, M. S. Hybertson, and R. Car, Nature (London) **396**, 58 (1998).
[2] Y. Tu and J. Tersoff, Phys. Rev. Lett. **89**, 86102 (2002).
[3] M. Di Ventra and S. T. Pantelides, Phys. Rev. Lett. **83**, 1624 (1999).
[4] S. Wang, M. DiVentra, S. G. Kim, and S. T. Pantelides, Phys. Rev. Lett. **86**, 5946 (2001).
[5] F. Amy, H. Enriquez, P. Soukiassian, P. F. Storino,Y. J. Chabal, A. J. Mayne, G. Dujardin, Y. K. Hwu, and C. Brylinski, Phys. Rev. Lett. **86**, 4342 (2001).
[6] H. Kobayashi, T. Sakurai, M. Takahashi, and Y. Nishioka, Phys. Rev. B **67**, 115305 (2003).
[7] I. Vickridge, I. Trimaille, J. J. Ganem, S. Rigo, C. Radtke, I. R. Baumvol, and F. C. Stedile, Phys. Rev. Lett. **89**, 256102 (2002).
[8] J. Dekker, K. Saarinen, H. O. Olafsson, and E. O. Sveinbjornson, Mater. Sci. Forum **433–436**, 543 (2003).
[9] N. S. Saks, S. S. Mani, and A. K. Agarwal, Appl. Phys. Lett. **76**, 2250 (2000).
[10] K. Fukuda, W. J. Cho, K. Arai, S. Suzuki, J. Senzaki, and T. Tanaka, Appl. Phys. Lett. **77**, 866 (2000).
[11] E. H. Poindexter, P. J. Caplan, B. E. Deal, and R. R. Razouk, J. Appl. Phys. **52**, 879 (1981).
[12] A. Stirling, A. Pasquarello, and J. C. Charlier, Phys. Rev. Lett. **85**, 2773 (2000).
[13] P. J. Macfarlane and M. E. Zvanut, J. Appl. Phys. **88**, 4122 (2000).
[14] Y. Shishkin, W. J. Choyke, and R. P. Devaty, Proceedings of the ICSCRM Conference, Lyon, 2003 [Mater. Sci. Forum (to be published)].
[15] J. L.Cantin, M. Schoisswohl, H. J.von Bardeleben, N. Hadj Zoubir, and M. Vergnat, Phys. Rev. B **52**, R11 599 (1995).
[16] V. Ya Bratus', S. S. Ishchenko, S. M. Okulov, I. P. Vorona, H. J. von Bardeleben, and M. Schoisswohl, Phys. Rev. B **50**, 15 449 (1994).
[17] J. Bourgoin and M. Lannoo, *Point Defects in Semiconductors II*, Springer Series in Solid State Sciences Vol. 35 (Springer Verlag, Berlin, 1981), p. 77.
[18] J. R. Morton and K. F. Preston, J. Magn. Reson. **30**, 577 (1978).
[19] M. A. Jupina and P. M. Lenahan, IEEE Trans. Nucl. Sci. **37**, 1650 (1990).
[20] A. Ekoué, O. Renault, T. Billon, L. DiCioccio, and G. Guillot, Mater. Sci. Forum **433–436**, 555 (2003).